Chemical Science

ROYAL SOCIETY OF CHEMISTRY

EDGE ARTICLE

View Article Online
View Journal | View Issue



Cite this: *Chem. Sci.*, 2025, **16**, 7544

All publication charges for this article have been paid for by the Royal Society of Chemistry

Received 23rd January 2025
Accepted 20th March 2025

DOI: 10.1039/d5sc00638d

rsc.li/chemical-science

# High-throughput microdroplet-based synthesis using automated array-to-array transfer†

Kai-Hung Huang, ‡[a] Kitmin Chen, ‡[a] Nicolás M. Morato, [ab] Thomas C. Sams, [a] Eric T. Dziekonski [a] and R. Graham Cooks *[ab]

Automation of chemical synthesis and high-throughput (HT) screening are important for speeding up drug discovery. Here, we describe an automated HT picomole scale synthesis system which uses desorption electrospray ionization (DESI) to create microdroplets of reaction mixtures at individual positions from a two-dimensional reactant array and transfer them to a corresponding position in an array of collected reaction products. On-the-fly chemical transformations are facilitated by the reaction acceleration phenomenon in microdroplets and high reaction conversions are achieved during the milliseconds droplet flight time from the reactant to the product array. Successful functionalization of bioactive molecules is demonstrated through the generation of 172 analogs (64% success rate) using multiple reaction types. Synthesis throughput is ~45 seconds/reaction including droplet formation, reaction, and collection steps, all of which occur in an integrated fashion, generating product amounts sufficient for subsequent bioactivity screening (low ng to low μg). Quantitative performance was validated using LC/MS. This system bridges the demonstrated capabilities of HT-DESI for reaction screening and label-free bioassays, allowing consolidation of the key early drug discovery steps around a single synthetic-analytical technology.



## Introduction

Rapid access to new molecules, an important part of drug discovery, is typically hindered by the time-consuming nature of traditional synthetic procedures.[1–3] This is especially relevant as, despite the increased development and implementation of high-throughput (HT) experimentation methodologies for reaction screening and biological activity testing,[3–5] those for automated synthesis are less well-developed with the exception of routes to peptides and oligonucleotides.[6–8] Substantial efforts are thus being made to develop automated synthetic systems for small molecules of a wide structural range,[9–15] although these new platforms often operate at a relatively large scale (mL) and relatively low throughput (hours per reaction).

Mass spectrometry (MS)-based techniques have emerged as powerful tools for HT reaction screening[16–26] as they can rapidly and automatically generate detailed reactivity data with special value as input for automated bioassay platforms and for machine learning algorithms to guide pathway selection. These advantages can be synergistically maximized when combined with the accelerated chemistry occurring in microdroplets, a strategy that provides both analytical (inherent to MS) and synthetic speed (due to the accelerated reactions). HT reaction screening (>1 Hz) by accelerated microdroplet reactions uses automated desorption electrospray ionization (DESI)[27,28] together with direct MS detection. In DESI, a pneumatically propelled solvent spray impacts the surface of the reaction mixture and releases secondary charged microdroplets. Accelerated reactions occur at their air-liquid interface.[29–36] The acceleration factor, expressed in terms of the ratio of rate constants in microdroplets relative to bulk, is in the range of $10^3$–$10^6$ and it is attributed to interfacial phenomena: the partial solvation of reagents,[37,38] the strong electric field at the droplet surface,[39–41] and the presence of highly reactive species (*i.e.* hydronium/hydroxide and redox species)[39,42,43] in this unique environment. HT-DESI-MS thus leverages microdroplet chemistry to provide information on screening outcomes rapidly and without the need for incubation of reaction mixtures,[25,26] yielding results comparable to those of slower screening approaches.[44] Despite achieving rapid screening by HT-DESI-MS,[45] the collection of reaction products by droplet-based synthesis is still constrained to non-automated, low throughput and large scale approaches.[36,46]

In this study, we demonstrate what appears to be the first small-scale HT synthesis in an array format through physical collection of the reaction products in the secondary DESI

[a]*Department of Chemistry, Purdue University, West Lafayette, Indiana 47907, USA. E-mail: cooks@purdue.edu*

[b]*Purdue Institute for Cancer Research, Purdue University, West Lafayette, Indiana 47907, USA*

† Electronic supplementary information (ESI) available: Experimental methods, prototype details, and product characterization. See DOI: https://doi.org/10.1039/d5sc00638d

‡ Authors contributed equally.

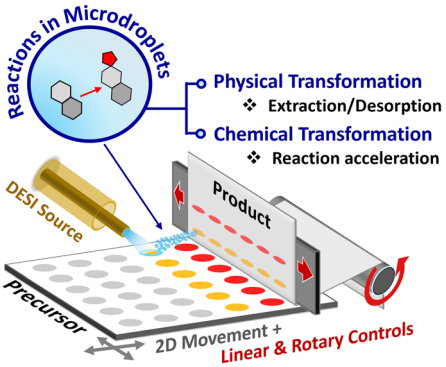


Fig. 1 Concept of array-to-array (reactants-to-products) transfer using DESI for high-throughput small-scale synthesis.

microdroplets. Collection of materials from a DESI spray without automation has been demonstrated with pure analytes one at a time,[47–49] however to do this in an autonomous HT fashion from a two-dimensional array of reagents, one must rapidly collect products of each reaction mixture at the corresponding position in a second array. This was accomplished by mimicking the movement mechanism of an old-fashioned typewriter, *i.e.* a linear motion across a single row and a rotary motion for row-to-row transitions. This mechanism allows for an array-to-array transfer system (Fig. 1) in which reagents on the sample surface (*i.e.* reactant or precursor array) undergo accelerated chemical transformations during the DESI droplet flight and land as reaction products on the collection surface (*i.e.* product array). Here we describe a prototype of this automated small-scale synthesis system and showcase its use for the late-stage diversification[50] of bioactive molecules.

## Results and discussion

The microdroplet-based array-to-array transfer system (Fig. 2A) is comprised of four main components: a homebuilt DESI sprayer, a precursor array module (XYZ moving stage for the reagent array), a product array module (collection system to hold the array of reaction products), and a controller that enables automated motion. The DESI sprayer is mounted on a stage capable of adjusting the position and angle at which the DESI spray impacts the material (*i.e.* reaction mixtures) pre-deposited on the precursor array. An Arduino controller orchestrates five independent motors enabling control over the movements of each component. The precursor array module allows three-dimensional movement: X and Y motions for rastering of the precursor array beneath the sprayer providing access to different array positions, and Z motion for adjusting the distance between the precursor array and the collection surface. The product array module uses two motions: linear translation, which enables access to various positions within a single row, and rotary motion, which advances between rows as in a typewriter roller. Custom software was used to control the automated array-to-array collection. Detailed description of the individual components and parameters can be found in the ESI (Section I and Fig. S1–S7).†

To qualitatively visualize desorption and collection for system evaluation, dye spots were deposited on the precursor

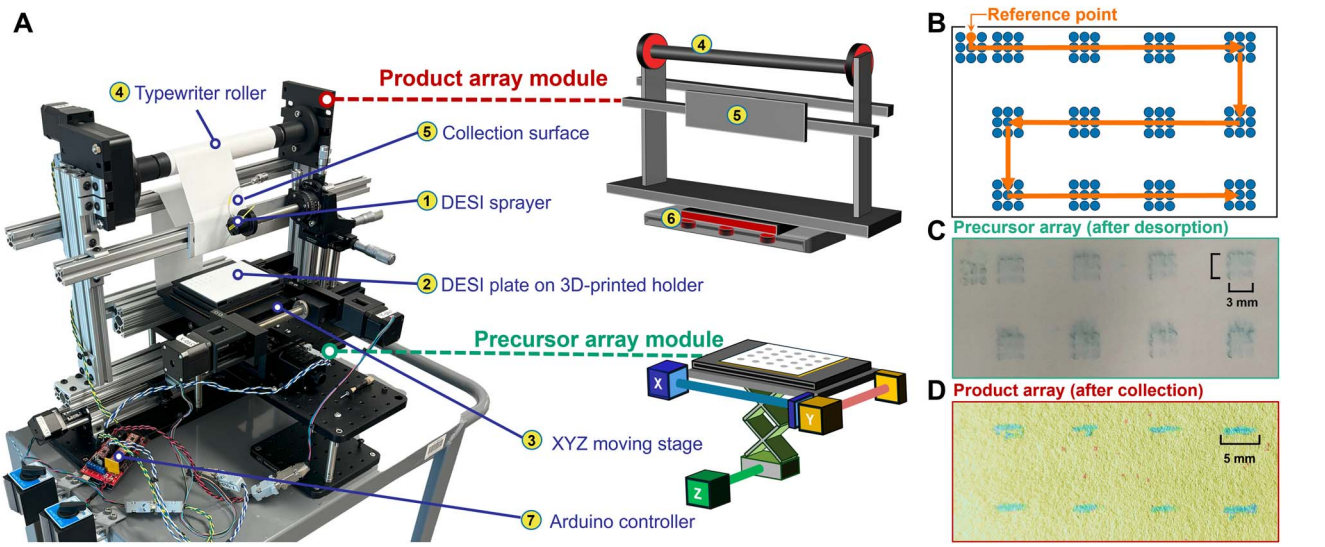


Fig. 2 Photograph of array-to-array transfer system. (A) Automated DESI synthesis device mounted on a cart. The DESI sprayer (1) is located on an adjustable mount. The precursor array (2) is secured on a 3D-printed holder mounted on a XYZ moving stage (3) controlled by three stepper motors. The typewriter-based product collection module is constructed of a platen roller (4) with a rotary motor that enables a continuous supply of chromatography paper, while a collector plate (5) provides structural support for the paper surface and a wheel/axle assembly (6) provides stable linear motion with a motor drive. All five separate stepper motors are connected to an Arduino controller (7), which is operated with homebuilt software. The automated movements (B) are customized for array-to-array transfer of material from each of the 9-spot (9 $mm^2$) square that constitute a single sample in this particular array. These squares, made up of 9 pinned blue dye spots on the precursor array (C), were desorbed and collected onto chromatography paper generating a product array of horizontal bands some 5 mm wide (D). (D) is contrast adjusted for better visualization.

array. In all experiments, 9 spots were used per sample to achieve 450 nL of reactant mixture deposited (50 nL per spot), and filter paper was used as collection surface. A custom motion pattern was utilized for the automated array-to-array collection (Fig. 2B), with the precursor array module moving in the *X*-axis to access and then raster across each sample (combined XY motion; see details in the ESI, Section I†). Simultaneously, the product array module moves linearly (X-dimension) and in sync in order to collect material in the corresponding array position, allowing for the collection of a single row of reactions. A new row for desorption and collection is then accessible *via* *Y*-axis motion of the precursor module and rotation of the collection module (platten roller), respectively. Note that there is active *Z*-axis control throughout the motion program, so that the precursor array is lowered during the new row access (in order to avoid cross-contamination) and then lifted again for collection. Automated repetition of these movements results in a two-dimensional array-to-array transfer, an old fashioned typewriter inspired strategy suitable for creating spatially resolved materials, as demonstrated by the desorption and DESI-mediated transfer of dye from spots in the precursor array (Fig. 2C) to corresponding positions in the product array (Fig. 2D). Note that the shape of the collected dye is attributed to the combined effects of the geometry of the 9-spot sample square and to gas dispersion of droplets along the surface plane.[47] A pure compound (neostigmine) was deposited on the precursor array to optimize the desorption efficiency using parameters such as movement step size, number of oscillations, and raster speed, all which can be readily modified using the custom control software. Details on this system optimization are provided in the ESI (Section II and Fig. S8).†

To quantitatively evaluate the synthetic efficiency of the automated system, we generated analogs of two bioactive compounds, 3-[(dimethylamino)methyl]phenol (S1, an acetylcholinesterase inhibitor precursor) and naloxone (S3, an opioid antagonist) *via* sulfonation and ene-type click reactions (Fig. 3A) using low μg amounts of starting materials. Collection efficiency was determined through analysis of extracted solutions from the collected materials using nanoelectrospray ionization (nESI) MS under non-accelerating analysis conditions (*i.e.* minimal droplet flight times so that no further chemical transformations could occur during the analysis). The relative ion ratio of the drug substrate or functionalized drug molecule to a structurally-similar internal standard (*i.e.* (S)-3-[1-(dimethylamino)ethyl]phenol and naltrexone for S1 and S3, respectively) was used to quantify the amount of reactant and product collected *via* an external calibration curve (Fig. 3B and Table S1†). Note that for selected reactions a second determination was carried out *via* liquid chromatography tandem MS (LC-MS/MS) to validate the direct nESI quantitative approach (see ESI, Section II, Fig. S10 and Table S2†). Across all reactions, the average collection efficiency (including products and reactants) achieved with the current prototype was 16 ± 7%. These modest collection efficiencies likely arise from the low takeoff angles (10°) of the secondary desorbed microdroplets,[51] the pneumatic obstruction generated by the collection surface, and the rapid spray divergence (see MS imaging results, Fig. 4A).

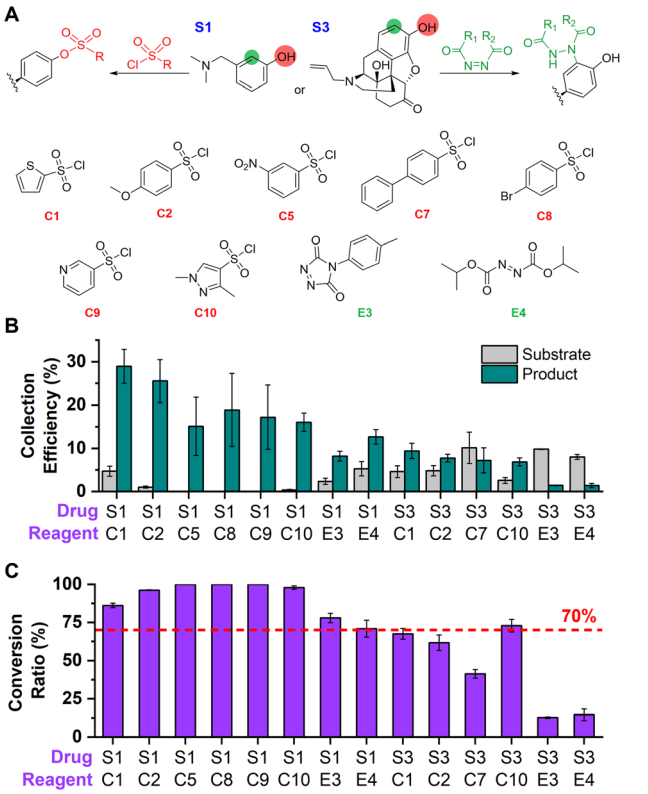


Fig. 3 Quantitative evaluation of the small-scale synthesis system. (A) Reaction scheme for sulfonation (red) and ene-type click reactions (green) using 3-[(dimethylamino)methyl]phenol (S1) and naloxone (S3) as substrates and sulfonyl chlorides or ene-reagents as functionalization reagents. The collection efficiencies for reactants and products (B) and the conversion ratios (C) for each reaction are also shown. In all cases the results represent the average of triplicate experiments with the error bars indicating standard deviations.

Due to the complexity of this secondary droplet generation, flight, and collection process,[51] further investigation and simulations might be required for collection optimization.

The efficiency of the accelerated chemical transformations in the DESI microdroplets was also evaluated by calculating conversion ratios (CR) for each reaction (see ESI, Section II†). Note that despite the inherent challenges in correlating CR and reaction yield that stem from ionization efficiency differences between substrates and products, CRs can still be used to semi-quantitatively assess reactivity trends for the functionalization of drug molecules. This is possible when performing late-stage functionalization of complex molecules, as often the most likely ionization site is preserved between the precursor drugs and their modified analogues. Here we demonstrate one such examples for the functionalization of S3 by comparison of CRs with LC-MS calculated yields (Table S2†). Additionally, the use of CRs is also useful when structurally similar products are generated through the same reaction type, as they will have comparable ionization efficiencies even though they differ systematically from those of their corresponding starting materials.

In most cases, the reactions explored showed high conversion (≥70%) and reproducibility (Fig. 3C). The combination of

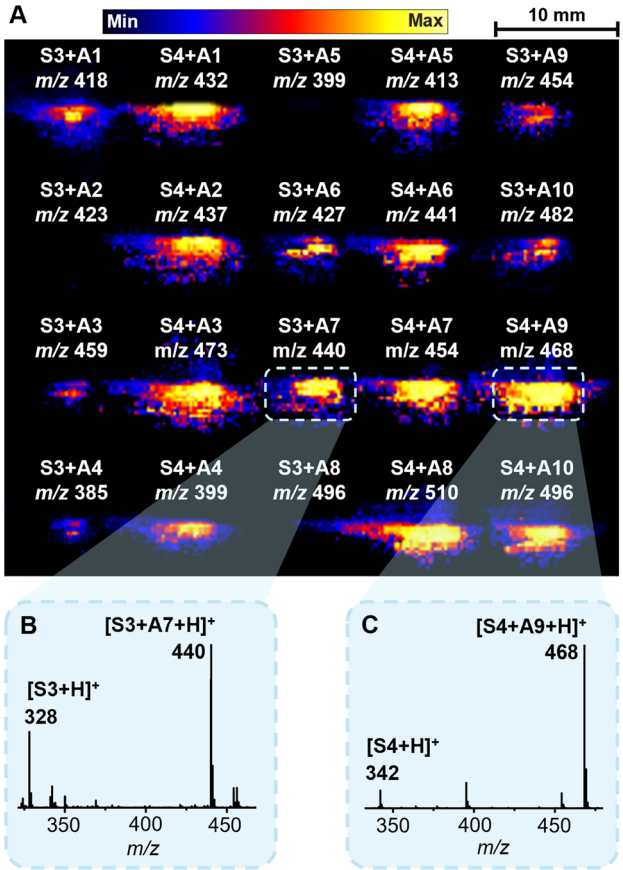


Fig. 4 MSI analysis of the product array generated using the HT-DESI-MS synthesis platform. (A) Composite ion images for all the functionalized forms naloxone (S3) and naltrexone (S4) obtained *via* imine formation (see details in the ESI†). Two representative mass spectra (obtained through averaging each spot region using MSI) are shown for the reactions of S3 + A7 (B) and S4 + A9 (C).

this high reaction efficiency with the modest collection efficiency achieved, allow for sufficient quantities of products to be generated (≥200 ng for all reactions except S3 + E3 and S3 + E4 in which the reaction conversions are low) for their subsequent biological activity screening, a task that can also be performed by HT-DESI-MS in a label-free manner.[52–55] It is worth highlighting that the amount of product collected can be adjusted (low ng to low μg scale) by varying the amount of reagent deposited on the precursor array or the DESI desorption time, which is readily controlled using the custom software.

Finally, the synthetic versatility of the HT-DESI-MS small-scale synthesis system was evaluated using a wide variety of chemical transformations together with *in situ* analysis of the collected product arrays using MS imaging (MSI). The substrates included small molecular building blocks, therapeutic agents and natural products (Fig. S17†), while the reactions explored were O/N-sulfonation, imine formation, reductive amination, fluorosulfurylation, thioesterification, $S_NAr$, *N*-alkylation, ene-type click reaction, and Katritzky transamination (Fig. S18–S24†). A total of 270 functionalizations were carried out using a throughput of ~45 seconds per transformation to prepare high-nanogram amounts of material. Note that accelerated reactions in microdroplets occur within tens to hundreds of milliseconds[56] (*i.e.* the flight time of the droplets from the precursor array to the product array), while the overall collection speed (5 seconds to 45 seconds, or longer) can be customized.

Through this experiment, a total of 172 reaction products were successfully synthesized (success rate: 64%) at nanogram scale in an array format, as confirmed by MSI (Fig. 4 and S19–S24†). For example, the spatial distribution and high conversion ratios across the product array from the functionalization of naloxone and naltrexone *via* imine formation can be visualized in the composed ion image of the reaction products (Fig. 4A) as well as the average mass spectra associated to each collected spot (Fig. 4B and C). In some cases, both reaction products and intermediates can be identified, as shown by the amine and imine analogs of androsterone (*via* reductive amination, Fig. S24†). Additionally, if isomeric products formed using isomeric alkylating reagents (*via* *N*-alkylation) or identical products formed using reagents with different leaving groups (*via* $S_NAr$) are collected, they are observed spatially separated, as expected (Fig. S22 and S23†). These MSI results illustrate the spatial resolution of the collection spot, typically 10 × 3 mm (w × h), with products mostly concentrated at the center. Note that the generated array of spatially-resolved functionalized products provides a clear integrative advantage for bioactivity screening, for instance using on-paper[57–59] or solution-based bioassays[53–55] coupled to HT-DESI-MS. In the former case, the paper substrate can be automatically analyzed after the biological reaction. In the latter, more widely applicable case, collected spots need to be transferred to standard well plates for incubation with the biological target. For this purpose, we designed a batch punching tool that allows for simultaneous cutting and transfer of the entire array of collected spots, onto a standard 96-well plate (Fig. S25†).

## Conclusions

As shown, we have developed a fully automated and customizable system for HT small-scale synthesis in an array-to-array fashion leveraging the unique feature of accelerated chemistry (millisecond reaction times) occurring in DESI microdroplets. This system successfully achieves simultaneous physical (desorption-collection) and chemical (reactants to products) transformation of arrays, and it is directly compatible with an existing automated HT-DESI-MS system[45] as it uses standard microplate-sized reactant plates as input. Integration within this platform will lead to a complete workflow involving (i) automated ultra-fast (~1 second per reaction) screening, (ii) online MS/MS structural confirmation (~5 seconds per reaction), and (iii) synthesis using the array-to-array collector only on the reactions deemed successful through the screening and whose product structures are confirmed (~45 seconds per reaction), leading to an overall screening-characterization-physical collection throughput of less than 1 minute. Despite the sequential synthesis step, this is a competitive throughput when compared to parallel synthesis coupled with traditional

LC-MS based screening, and it results in a more efficient process less prone to generation of negative synthetic results (*i.e.* unsuccessful reactions that were nonetheless prepared, incubated and characterized) due to the multi-stage evaluation workflow proposed here.

Under our current settings, high nanogram amounts of reaction products are collected with a throughput of ~45 seconds per transformation in reactions exhibiting high CR (>70%) despite modest collection efficiencies (~16%). Nevertheless, all these parameters are currently being improved through system modifications. Note that the fastest throughput accessible is 5 seconds per reaction (a single ~800 μm reactant spot), with sample consumption just 50 nL (picomole scale). The utility of this automated system was demonstrated with a wide range of substrates and reaction types through 172 successful chemical transformations collected in a spatially resolved array format. The products of the DESI reactions were readily analyzed by spot extraction or *in situ* MSI, showcasing the potential coupling of this synthetic system with subsequent biological activity screening *via* in-solution[53–55] or on-surface bioassays.[57–59]

## Data availability

All data on which this publication is based is given in the main text or ESI.†

## Author contributions

Dr R. G. Cooks and K.-H. Huang designed the experiments. Dr K.-H. Huang, K. Chen, Dr N. M. Morato, T. Sams, Dr E. T. Dziekonski performed the experiments. Dr R. G. Cooks, Dr K.-H. Huang, K. Chen, and Dr N. M. Morato wrote the manuscript.

## Conflicts of interest

There are no conflicts to declare.

## Acknowledgements

This work was supported by the National Center for Advancing Translational Sciences (NCATS) New Chemistries for Undrugged Targets through ASPIRE Collaborative Research Program (UG3/UH3 TR004139) and the Multi-University Research Initiative (MURI; grant FA9550-21-1-0170) sponsored by the Air Force Office of Scientific Research (AFOSR) *via* Stanford University (sub-award 62741613-204669). The authors acknowledge the use of the Purdue HT-DESI-MS Facility and the LC-MS platform at the Metabolite Profiling Facility (MPF) from the Bindley Bioscience Center, a core facility of the NIH-funded Indiana CTSI. Support from the Purdue Institute for Cancer Research (NIH P30 CA023168) is also gratefully acknowledged. The authors thank Wen Xiu for his assistance with the purification of selected synthesized products.

## References

1 P. G. Polishchuk, T. I. Madzhidov and A. Varnek, Estimation of the Size of Drug-like Chemical Space Based on GDB-17 Data, *J. Comput.-Aided Mol. Des.*, 2013, **27**(8), 675–679, DOI: 10.1007/s10822-013-9672-4.

2 W. A. Warr, M. C. Nicklaus, C. A. Nicolaou and M. Rarey, Exploration of Ultralarge Compound Collections for Drug Discovery, *J. Chem. Inf. Model.*, 2022, **62**(9), 2021–2034, DOI: 10.1021/acs.jcim.2c00224.

3 P. S. Gromski, A. B. Henson, J. M. Granda and L. Cronin, How to Explore Chemical Space Using Algorithms and Automation, *Nat. Rev. Chem*, 2019, **3**(2), 119–128, DOI: 10.1038/s41570-018-0066-y.

4 G. Schneider, Automating Drug Discovery, *Nat. Rev. Drug Discovery*, 2018, **17**(2), 97–113, DOI: 10.1038/nrd.2017.232.

5 C. J. Welch, High Throughput Analysis Enables High Throughput Experimentation in Pharmaceutical Process Research, *React. Chem. Eng.*, 2019, **4**(11), 1895–1911, DOI: 10.1039/C9RE00234K.

6 O. J. Plante, E. R. Palmacci and P. H. Seeberger, Automated Solid-Phase Synthesis of Oligosaccharides, *Science*, 2001, **291**(5508), 1523–1527, DOI: 10.1126/science.1057324.

7 R. B. Merrifield, Automated Synthesis of Peptides: Solid-Phase Peptide Synthesis, a Simple and Rapid Synthetic Method, Has Now Been Automated, *Science*, 1965, **150**(3693), 178–185, DOI: 10.1126/science.150.3693.178.

8 M. H. Caruthers, Gene Synthesis Machines: DNA Chemistry and Its Uses, *Science*, 1985, **230**(4723), 281–285, DOI: 10.1126/science.3863253.

9 A. G. Godfrey, T. Masquelin and H. Hemmerle, A Remote-Controlled Adaptive Medchem Lab: An Innovative Approach to Enable Drug Discovery in the 21st Century, *Drug Discovery Today*, 2013, **18**(17–18), 795–802, DOI: 10.1016/j.drudis.2013.03.001.

10 J. Li, S. G. Ballmer, E. P. Gillis, S. Fujii, M. J. Schmidt, A. M. E. Palazzolo, J. W. Lehmann, G. F. Morehouse and M. D. Burke, Synthesis of Many Different Types of Organic Small Molecules Using One Automated Process, *Science*, 2015, **347**(6227), 1221–1226, DOI: 10.1126/science.aaa5414.

11 A. Baranczak, N. P. Tu, J. Marjanovic, P. A. Searle, A. Vasudevan and S. W. Djuric, Integrated Platform for Expedited Synthesis–Purification–Testing of Small Molecule Libraries, *ACS Med. Chem. Lett.*, 2017, **8**(4), 461–465, DOI: 10.1021/acsmedchemlett.7b00054.

12 J. M. Granda, L. Donina, V. Dragone, D.-L. Long and L. Cronin, Controlling an Organic Synthesis Robot with Machine Learning to Search for New Reactivity, *Nature*, 2018, **559**(7714), 377–381, DOI: 10.1038/s41586-018-0307-8.

13 A.-C. Bédard, A. Adamo, K. C. Aroh, M. G. Russell, A. A. Bedermann, J. Torosian, B. Yue, K. F. Jensen and T. F. Jamison, Reconfigurable System for Automated Optimization of Diverse Chemical Reactions, *Science*, 2018, **361**(6408), 1220–1225, DOI: 10.1126/science.aat0650.

14 S. Rohrbach, M. Šiaučiulis, G. Chisholm, P.-A. Pirvan, M. Saleeb, S. H. M. Mehr, E. Trushina, A. I. Leonov,

G. Keenan, A. Khan, A. Hammer and L. Cronin, Digitization and Validation of a Chemical Synthesis Literature Database in the ChemPU, *Science*, 2022, **377**(6602), 172–180, DOI: 10.1126/science.abo0058.

15 B. Burger, P. M. Maffettone, V. V. Gusev, C. M. Aitchison, Y. Bai, X. Wang, X. Li, B. M. Alston, B. Li, R. Clowes, N. Rankin, B. Harris, R. S. Sprick and A. I. Cooper, A Mobile Robotic Chemist, *Nature*, 2020, **583**(7815), 237–241, DOI: 10.1038/s41586-020-2442-2.

16 A. B. Santanilla, E. L. Regalado, T. Pereira, M. Shevlin, K. Bateman, L. C. Campeau, J. Schneeweis, S. Berritt, Z. C. Shi, P. Nantermet, Y. Liu, R. Helmy, C. J. Welch, P. Vachal, I. W. Davies, T. Cernak and S. D. Dreher, Nanomole-Scale High-Throughput Chemistry for the Synthesis of Complex Molecules, *Science*, 2015, **347**(6217), 49–53, DOI: 10.1126/science.1259203.

17 S. Lin, S. Dikler, W. D. Blincoe, R. D. Ferguson, R. P. Sheridan, Z. Peng, D. V. Conway, K. Zawatzky, H. Wang, T. Cernak, I. W. Davies, D. A. DiRocco, H. Sheng, C. J. Welch and S. D. Dreher, Mapping the Dark Space of Chemical Reactions with Extended Nanomole Synthesis and MALDI-TOF MS, *Science*, 2018, **361**(6402), eaar6236, DOI: 10.1126/science.aar6236.

18 K. J. DiRico, W. Hua, C. Liu, J. W. Tucker, A. S. Ratnayake, M. E. Flanagan, M. D. Troutman, M. C. Noe and H. Zhang, Ultra-High-Throughput Acoustic Droplet Ejection-Open Port Interface-Mass Spectrometry for Parallel Medicinal Chemistry, *ACS Med. Chem. Lett.*, 2020, **11**(6), 1101–1110, DOI: 10.1021/acsmedchemlett.0c00066.

19 A. A. Bayly, B. R. McDonald, M. Mrksich and K. A. Scheidt, High-Throughput Photocapture Approach for Reaction Discovery, *Proc. Natl. Acad. Sci. U.S.A.*, 2020, **117**(24), 13261–13266, DOI: 10.1073/pnas.2003347117.

20 D. Perera, J. W. Tucker, S. Brahmbhatt, C. J. Helal, A. Chong, W. Farrell, P. Richardson and N. W. Sach, A Platform for Automated Nanomole-Scale Reaction Screening and Micromole-Scale Synthesis in Flow, *Science*, 2018, **359**(6374), 429–434, DOI: 10.1126/science.aap9112.

21 M. Wleklinski, B. P. Loren, C. R. Ferreira, Z. Jaman, L. Avramova, T. J. Paschoal Sobreira, D. H. Thompson and R. G. Cooks, High Throughput Reaction Screening Using Desorption Electrospray Ionization Mass Spectrometry, *Chem. Sci.*, 2018, **9**(6), 1647–1653, DOI: 10.1039/c7sc04606e.

22 E. E. Kempa, K. A. Hollywood, C. A. Smith and P. E. Barran, High Throughput Screening of Complex Biological Samples with Mass Spectrometry-from Bulk Measurements to Single Cell Analysis, *Analyst*, 2019, **144**(3), 872–891, DOI: 10.1039/c8an01448e.

23 F. Pu, N. L. Elsen and J. D. Williams, Emerging Chromatography-Free High-Throughput Mass Spectrometry Technologies for Generating Hits and Leads, *ACS Med. Chem. Lett.*, 2020, **11**(11), 2108–2113, DOI: 10.1021/acsmedchemlett.0c00314.

24 A. C. Sun, D. J. Steyer, R. I. Robinson, C. Ginsburg-Moraff, S. Plummer, J. Gao, J. W. Tucker, D. Alpers, C. R. J. Stephenson and R. T. Kennedy, High-Throughput Optimization of Photochemical Reactions Using Segmented-Flow Nanoelectrospray-Ionization Mass Spectrometry, *Angew. Chem., Int. Ed.*, 2023, **62**(28), e202301664, DOI: 10.1002/anie.202301664.

25 K.-H. Huang, N. M. Morato, Y. Feng and R. G. Cooks, High-Throughput Diversification of Complex Bioactive Molecules by Accelerated Synthesis in Microdroplets, *Angew. Chem., Int. Ed.*, 2023, **62**(22), e202300956, DOI: 10.1002/anie.202300956.

26 K.-H. Huang, N. M. Morato, Y. Feng, A. Toney and R. G. Cooks, Rapid Exploration of Chemical Space by High-Throughput Desorption Electrospray Ionization Mass Spectrometry, *J. Am. Chem. Soc.*, 2024, jacs.4c11037, DOI: 10.1021/jacs.4c11037.

27 Z. Takáts, J. M. Wiseman, B. Gologan and R. G. Cooks, Mass Spectrometry Sampling Under Ambient Conditions with Desorption Electrospray Ionization, *Science*, 2004, **306**(5695), 471–473, DOI: 10.1126/science.1104404.

28 N. M. Morato and R. G. Cooks, Desorption Electrospray Ionization Mass Spectrometry: 20 Years, *Acc. Chem. Res.*, 2023, **56**(18), 2526–2536, DOI: 10.1021/acs.accounts.3c00382.

29 Z. Wei, Y. Li, R. G. Cooks and X. Yan, Accelerated Reaction Kinetics in Microdroplets: Overview and Recent Developments, *Annu. Rev. Phys. Chem.*, 2020, **71**(1), 31–51, DOI: 10.1146/ANNUREV-PHYSCHEM-121319-110654.

30 S. Banerjee and R. N. Zare, Syntheses of Isoquinoline and Substituted Quinolines in Charged Microdroplets, *Angew. Chem., Int. Ed.*, 2015, **54**(49), 14795–14799, DOI: 10.1002/anie.201507805.

31 W. Wang, L. Qiao, J. He, Y. Ju, K. Yu, G. Kan, C. Guo, H. Zhang and J. Jiang, Water Microdroplets Allow Spontaneously Abiotic Production of Peptides, *J. Phys. Chem. Lett.*, 2021, **12**(24), 5774–5780, DOI: 10.1021/acs.jpclett.1c01083.

32 A. J. Grooms, A. N. Nordmann and A. K. Badu-Tawiah, Dual Tunability for Uncatalyzed N-Alkylation of Primary Amines Enabled by Plasma-Microdroplet Fusion, *Angew. Chem., Int. Ed.*, 2023, **135**(51), e202311100, DOI: 10.1002/anie.202311100.

33 X. Zhong, H. Chen and R. N. Zare, Ultrafast Enzymatic Digestion of Proteins by Microdroplet Mass Spectrometry, *Nat. Commun.*, 2020, **11**(1), 1–9, DOI: 10.1038/s41467-020-14877-x.

34 W. Zhang, B. Zheng, X. Jin, H. Cheng and J. Liu, Rapid Epoxidation of α,β-Unsaturated Olefin in Microdroplets without Any Catalysts, *ACS Sustain. Chem. Eng.*, 2019, **7**(17), 14389–14393, DOI: 10.1021/acssuschemeng.9b04059.

35 Z. Song, C. Liang, K. Gong, S. Zhao, X. Yuan, X. Zhang and J. Xie, Harnessing the High Interfacial Electric Fields on Water Microdroplets to Accelerate Menshutkin Reactions, *J. Am. Chem. Soc.*, 2023, **145**(48), 26003–26008, DOI: 10.1021/jacs.3c11650.

36 L. Xue, B. Zheng, J. Sun, J. Liu and H. Cheng, Water Microdroplet Chemistry for Accelerating Green Thiocyanation and Discovering Water-Controlled Divergence, *ACS Sustain. Chem. Eng.*, 2023, **11**(34), 12780–12789, DOI: 10.1021/acssuschemeng.3c03313.

37 L. Qiu, Z. Wei, H. Nie and R. G. Cooks, Reaction Acceleration Promoted by Partial Solvation at the Gas/Solution Interface, *ChemPlusChem*, 2021, **86**(10), 1362–1365, DOI: 10.1002/CPLU.202100373.

38 K. D. Judd, S. W. Parsons, D. B. Eremin, V. V. Fokin and J. M. Dawlaty, Visualizing Partial Solvation at the Air–Water Interface, *Chem. Sci.*, 2024, **15**(22), 8346–8354, DOI: 10.1039/D4SC01311E.

39 J. K. Lee, K. L. Walker, H. S. Han, J. Kang, F. B. Prinz, R. M. Waymouth, H. G. Nam and R. N. Zare, Spontaneous Generation of Hydrogen Peroxide from Aqueous Microdroplets, *Proc. Natl. Acad. Sci. U.S.A.*, 2019, **116**(39), 19294–19298, DOI: 10.1073/pnas.1911883116.

40 H. Xiong, J. K. Lee, R. N. Zare and W. Min, Strong Electric Field Observed at the Interface of Aqueous Microdroplets, *J. Phys. Chem. Lett.*, 2020, **11**(17), 7423–7428, DOI: 10.1021/acs.jpclett.0c02061.

41 H. Hao, I. Leven and T. Head-Gordon, Can Electric Fields Drive Chemistry for an Aqueous Microdroplet?, *Nat. Commun.*, 2022, **13**(1), 1–8, DOI: 10.1038/s41467-021-27941-x.

42 J. P. Heindel, H. Hao, R. A. LaCour and T. Head-Gordon, Spontaneous Formation of Hydrogen Peroxide in Water Microdroplets, *J. Phys. Chem. Lett.*, 2022, **13**(43), 10035–10041, DOI: 10.1021/acs.jpclett.2c01721.

43 L. Qiu and R. G. Cooks, Spontaneous Oxidation in Aqueous Microdroplets: Water Radical Cation as Primary Oxidizing Agent, *Angew. Chem., Int. Ed.*, 2024, **63**(17), e202400118, DOI: 10.1002/anie.202400118.

44 D. L. Logsdon, Y. Li, T. J. Paschoal Sobreira, C. R. Ferreira, D. H. Thompson and R. G. Cooks, High-Throughput Screening of Reductive Amination Reactions Using Desorption Electrospray Ionization Mass Spectrometry, *Org. Process Res. Dev.*, 2020, **24**(9), 1647–1657, DOI: 10.1021/acs.oprd.0c00230.

45 N. M. Morato, M. P. T. Le, D. T. Holden and R. G. Cooks, Automated High-Throughput System Combining Small-Scale Synthesis with Bioassays and Reaction Screening, *SLAS Technol.*, 2021, **26**(6), 555–571, DOI: 10.1177/24726303211047839.

46 C. Liu, J. Li, H. Chen and R. N. Zare, Scale-up of Microdroplet Reactions by Heated Ultrasonic Nebulization, *Chem. Sci.*, 2019, **10**(40), 9367–9373, DOI: 10.1039/c9sc03701b.

47 A. R. Venter, A. Kamali, S. Jain and S. Bairu, Surface Sampling by Spray-Desorption Followed by Collection for Chemical Analysis, *Anal. Chem.*, 2010, **82**(5), 1674–1679, DOI: 10.1021/ac902013x.

48 S. Jain, A. Heiser and A. R. Venter, Spray Desorption Collection: An Alternative to Swabbing for Pharmaceutical Cleaning Validation, *Analyst*, 2011, **136**(7), 1298, DOI: 10.1039/c0an00728e.

49 A. S. Kamali, J. G. Thompson, S. Bertman, J. B. Miller and A. R. Venter, Spray Desorption Collection of Free Fatty Acids onto a Solid Phase Microextraction Fiber for Trap Grease Analysis in Biofuel Production, *Anal. Methods*, 2011, **3**(3), 683, DOI: 10.1039/c0ay00567c.

50 K. E. Kim, A. N. Kim, C. J. McCormick and B. M. Stoltz, Late-Stage Diversification: A Motivating Force in Organic Synthesis, *J. Am. Chem. Soc.*, 2021, **143**(41), 16890–16901, DOI: 10.1021/JACS.1C08920/ASSET/IMAGES/LARGE/JA1C08920_0004.JPEG.

51 A. B. Costa and R. G. Cooks, Simulated Splashes: Elucidating the Mechanism of Desorption Electrospray Ionization Mass Spectrometry, *Chem. Phys. Lett.*, 2008, **464**(1–3), 1–8, DOI: 10.1016/j.cplett.2008.08.020.

52 R. G. Cooks, Y. Feng, K.-H. Huang, N. M. Morato and L. Qiu, Re-Imagining Drug Discovery Using Mass Spectrometry, *Isr. J. Chem.*, 2023, **63**(7–8), e202300034, DOI: 10.1002/ijch.202300034.

53 N. M. Morato, D. T. Holden and R. G. Cooks, High-Throughput Label-Free Enzymatic Assays Using Desorption Electrospray-Ionization Mass Spectrometry, *Angew. Chem., Int. Ed.*, 2020, **59**(46), 20459–20464, DOI: 10.1002/anie.202009598.

54 S. C. Kulathunga, N. M. Morato, Q. Zhou, R. G. Cooks and A. D. Mesecar, Desorption Electrospray Ionization Mass Spectrometry Assay for Label-Free Characterization of SULT2B1b Enzyme Kinetics, *ChemMedChem*, 2022, **17**(9), e202200043, DOI: 10.1002/CMDC.202200043.

55 Y. Feng, N. M. Morato, K.-H. Huang, M. Lin and R. G. Cooks, High-Throughput Label-Free Opioid Receptor Binding Assays Using an Automated Desorption Electrospray Ionization Mass Spectrometry Platform, *Chem. Commun.*, 2024, **60**(63), 8224–8227, DOI: 10.1039/D4CC02346C.

56 A. Venter, P. E. Sojka and R. G. Cooks, Droplet Dynamics and Ionization Mechanisms in Desorption Electrospray Ionization Mass Spectrometry, *Anal. Chem.*, 2006, **78**(24), 8549–8555, DOI: 10.1021/ac0615807.

57 D. O. Carmany, P. M. Mach, G. M. Rizzo, E. S. Dhummakupt, E. M. McBride, J. W. Sekowski, B. Benton, P. S. Demond, M. W. Busch and T. Glaros, On-Substrate Enzymatic Reaction to Determine Acetylcholinesterase Activity in Whole Blood by Paper Spray Mass Spectrometry, *J. Am. Soc. Mass Spectrom.*, 2018, **29**(12), 2436–2442, DOI: 10.1007/s13361-018-2072-1.

58 K. E. Boehle, C. S. Carrell, J. Caraway and C. S. Henry, Paper-Based Enzyme Competition Assay for Detecting Falsified β-Lactam Antibiotics, *ACS Sens.*, 2018, **3**(7), 1299–1307, DOI: 10.1021/acssensors.8b00163.

59 K. Talalak, J. Noiphung, T. Songjaroen, O. Chailapakul and W. Laiwattanapaisal, A Facile Low-Cost Enzymatic Paper-Based Assay for the Determination of Urine Creatinine, *Talanta*, 2015, **144**, 915–921, DOI: 10.1016/j.talanta.2015.07.040.